



1 **An improved method for calculating regional crop water footprint based on**
2 **hydrological process analysis**

3
4 **Luan Xiao-Bo^{1,2,#}, Yin Ya-Li^{3,#}, Wu Pu-Te^{2,3,*}, Sun Shi-Kun^{1,3,*}, Wang Yu-Bao^{1,3}, Gao Xue-Rui³,**
5 **Liu Jing⁴**

6 ¹ Institute of Water Saving Agriculture in Arid regions of China, Northwest A&F University, Yangling,
7 Shaanxi 712100, China

8 ² Institute of Soil and Water Conservation, Chinese Academy of Sciences and Ministry of Water
9 Resources, Yangling, Shaanxi 712100, China

10 ³ Key Laboratory of Agricultural Soil and Water Engineering in Arid and Semiarid Areas, Ministry of
11 Education, Northwest A&F University, Yangling, Shaanxi 712100, China

12 ⁴ College of Hydrology and Water Resources, Hohai University, Nanjing, Jiangsu 210098, China

13

14 # Luan Xiao-Bo and Yin Ya-Li contributed equally to this work.

15 * Corresponding Author:

16 Wu Pu-Te (gjzwpt@vip.sina.com) and Sun Shi-Kun (sksun@nwafu.edu.cn)

17 **Address:** Institute of Soil and Water Conservation, Chinese Academy of Sciences and Ministry of
18 Water Resources, Yangling 712100, Shaanxi, China



19 **Abstract**

20 Fresh water is consumed during agricultural production. With the shortage of water resources,
21 assessing the water use efficiency is crucial to effectively managing agricultural water resources. The
22 water footprint is a new index for water use evaluation, and it can reflect the quantity and types of
23 water usage during crop growth. This study aims to establish a method for calculating the region-scale
24 water footprint of crop production based on hydrological processes. This method analyzes the
25 water-use process during the growth of crops, which includes irrigation, precipitation, underground
26 water, evapotranspiration, and drainage, and it ensures a more credible evaluation of water use. As
27 illustrated by the case of the Hetao irrigation district (HID), China, the water footprints of wheat, corn
28 and sunflower were calculated using this method. The results show that canal water loss and
29 evapotranspiration were responsible for most of the water consumption and accounted for 47.9% and
30 41.8% of the total consumption, respectively. The total water footprints of wheat, sunflower and corn
31 were 1380-2888 m³/t, 942-1774 m³/t, and 2095-4855 m³/t, respectively, and the blue footprint accounts
32 for more than 86%. The spatial distribution pattern of the green, blue and total water footprint for the
33 three crops demonstrated that higher values occurred in the eastern part of the HID, which had more
34 precipitation and was further from the irrigating gate. This study offers a vital reference for improving
35 the method used to calculate the crop water footprint.

36 **Key words**

37 SWAT model; Regional Scale; Water use process; Hetao irrigation district



38 **1 Introduction**

39 Human activities and climate change have serious effects on the availability of water resources
40 (Nijssen et al., 2001; Haddeland et al., 2014). Agricultural production is major consumer of global
41 water resources and accounts for 85% of the global blue water (surface or groundwater) consumption
42 (Shiklomanov, 2000; Vörösmarty et al., 2010). In China, 63% of all water is used for agricultural
43 production each year, and the area of irrigated farmland is 39.6% of the total arable land. Irrigation is
44 the key to ensuring agricultural production (NBSC, 2016). With the rapid development of China's
45 economy, the demand for water has increased in industrial production and in the lives of residents (Duh
46 et al., 2008; Liu et al., 2008; Bao and Fang, 2012). Environmental pollution reduces water availability
47 (Jiang, 2009; Schwarzenbach et al., 2010) and these changes place great pressure on regional water
48 resources (Piao et al., 2010; Wang et al., 2014); meanwhile, climate change aggravates the situation
49 (Elliott et al., 2014; Sun et al., 2018). With limited water resources, economic demand for water will
50 inevitably and gradually take up the agricultural water use, which is a challenge for maintaining steady
51 agricultural production (Chen, 2007; Khan et al., 2009), especially in the dry areas of northern China
52 (Deng et al., 2006; Du et al., 2014). Strengthening agricultural water management and improving water
53 use efficiency are significant aspects of handling water scarcity, and a reasonable evaluation of the
54 water resource utilization of crop production is the premise for developing an agricultural water
55 management plan and implementing water saving measures. Therefore, how to precisely evaluate the
56 effective utilization ratio of current agricultural water use, improve the utilization efficiency, and
57 reduce the negative impact of the reduction of available agricultural water is an important issue that all
58 countries need to address Globally, this is also of vital importance for ensuring food production and
59 reducing the pressure on water resources. The water footprint theory provides new insights and ideas to



60 solve these problems (Hoekstra, 2003). The water footprint is an indicator of freshwater use and can be
61 used to quantify water consumption throughout the production supply chain. It reflects the amount of
62 water and types of resources that are consumed (Hoekstra, 2011). In the agricultural sector, it can also
63 be used to evaluate whether a crop's water footprint is reasonable and whether it varies regionally.
64 Because green water can be exploited, measures need to be taken to reduce the water footprints of crop
65 production, especially to decrease the blue water consumption to mitigate the demand for blue water in
66 agriculture. The accurate and precise quantification of crop water footprints is the premise to achieving
67 the above goals.

68 Currently, many scholars have quantified various levels of crop water footprints and Hoekstra et al.
69 (2011) put out two main methods for calculating the crop water footprint. The first method is the crop
70 water requirement method. This method simulates the evapotranspiration (ET) of crops under optimal
71 conditions with the ET calculated by the Penman-Monteith Equation (Allen et al., 1998) and the
72 effective precipitation calculation provided by the United States Department of Agriculture Soil
73 Conservation Service (USDA SCS) (USDA, 1994). The green water ET is the smaller value of total
74 crop ET and effective precipitation. The blue water ET is obtained through the difference between the
75 total crop ET and effective precipitation. Finally, when combined with crop yields, the crop blue and
76 green water footprint can be calculated. The second method is the irrigation schedule method. This
77 method is based on an empirical formula model such as the CROPWAT model (FAO, 2010) and the
78 AQUACROP model (Pasquale et al., 2009). These methods can simulate crop ET throughout the
79 growing period according to the soil water balance under optimal or suboptimal conditions. The blue
80 water footprint is the smaller value of net irrigation water and the actual irrigation water requirement.
81 The green water ET is equal to the total ET minus blue water. Both of the above methods are based on



82 empirical formulas. A few scholars have attempted to calculate the region-scale water footprints, for
83 example, Sun et al. (2013b) used the difference between diversion and drainage to calculate the water
84 footprint of crop production in irrigated areas. However, these methods have certain shortages, which
85 are as follows:

86 First, the empirical methods have not determined the applicability; i.e., the method is applicable to
87 a field-scale or region-scale water footprint calculation. These methods calculated the field-scale water
88 footprint with net irrigation water considered as irrigation water, and without considering water loss
89 during transport or drainage, which definitely serve for crop growth. Therefore, these methods are
90 field-scale methods, whereas a region-scale method should include the above two losses. Presently,
91 irrigation water is mainly consumed by irrigated agriculture, and the current methods have not included
92 water loss during transport and drainage. Therefore, the field-scale water footprint calculation does not
93 precisely apply to irrigated agriculture, but few region-scale methods of have been established.

94 Second, the irrigation data in these methods are simulation values and not based on the actual
95 irrigation time and irrigation quota; therefore, these data cannot reflect the real situation of the local
96 water usage due to the incorrect simulation data. At the same time, these methods cannot distinguish
97 the source of the crop water, for instance, whether it is from precipitation, surface water or
98 groundwater.

99 Third, the current region-scale method has not been appropriately established. The method that
100 Sun et al. (2013b) used had certain limits. It included all of the water consumption, but it could not
101 distinguish the specific source of blue water from canal loss, field ET or groundwater. Due to its low
102 spatial resolution, only the water footprint of the entire irrigated area could be calculated instead of the
103 difference inside this area.



104 Agricultural production water covers the diversion - transportation - irrigation - drainage and
105 precise calculation of the above processes and the premise of quantifying crops' water footprints.
106 Currently, most studies focus on the field scale and lack systematic evaluation on the whole process of
107 water consumption during crop growth. To overcome this problem, this study puts forward an
108 improved region-scale calculation method of the crop water footprint based on hydrological process
109 analysis and used it to quantify the crop water footprint in HID. This method based on physical
110 hydrological model (SWAT), simulated the regional hydrologic cycle process, which obtained the water
111 consumption and the field drainage, calculated the water loss during delivery using the water
112 conveyance efficiency of the canal, and then quantified the region-scale crop water footprint using the
113 yields of the crops. This method will provide comprehensive information for the water resource
114 consumption process in the analysis of crop production links and improve the spatial resolution of
115 quantifying the crops' water footprint.

116 **2 Materials and methods**

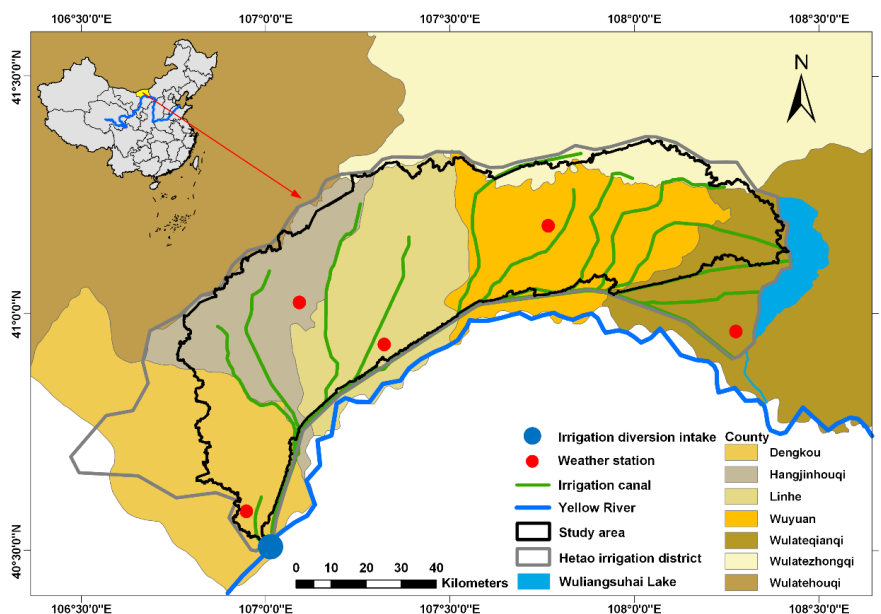
117 **2.1 Study site**

118 The Hetao irrigation district (HID) is located in the middle of the Yellow River basin in western
119 Inner Mongolia (Fig. 1) and is one of the three largest irrigation districts in China. The HID has a
120 continental monsoon climate with the lowest temperature in January (average -10°C) and highest
121 temperature in July (average 23°C). The annual average precipitation is 180 mm and annual potential
122 evaporation is 220 mm. The area of the HID is $1.12 \times 10^4 \text{ km}^2$.

123 Irrigation water is diverted from the Yellow River. The irrigation and drainage systems in the HID
124 are composed of irrigation canals and drainage ditches; the irrigation system has a general main canal
125 (228.9 km) and 12 main canals (total 755 km), and the drainage system has a general main ditch (227



126 km) and 12 main ditches (total 523 km). The main crops include wheat, corn and sunflower (Fig. 1).



127

128 **Fig. 1.** Location of the Hetao Irrigation District (HID) in China

129 2.2 Model description

130 The SWAT (soil and water assessment tool) model is a semi-distributed physical hydrological
131 model. The model was developed by USDA Agricultural Research Center and it used climate, soil,
132 topography, plants and land management practices to simulate hydrologic, sediment, crop growth and
133 nutrient cycle. The model partitions a watershed into sub-basins by topography and then partitions the
134 sub-basins into hydrologic response units (HRU) based on soil type and land use to assess soil erosion,
135 non-point pollution, and hydrologic processes (Haverkamp et al., 2002). The water balance equation
136 governed by the hydrologic component of the SWAT model (Neitsch et al., 2011) is as follows:

$$137 \quad SW_t = SW_0 + \sum_{i=1}^t (R_{day} - Q_{surf} - E_a - W_{seep} - Q_{gw}) \quad (1)$$

138 where SW_t is the final soil water content (mm H₂O), SW_0 is the initial soil water content (mm H₂O),



139 t is the time (days), R_{day} is the amount of precipitation on day i (mm H₂O), Q_{surf} is the amount of
140 surface runoff on day i (mm H₂O), E_a is the amount of actual ET on day i (mm H₂O), W_{seep} is the
141 amount of percolation and bypass flow exiting the bottom of the soil profile on day i (mm H₂O), and
142 Q_{gw} is the amount of return flow on day i (mm H₂O).

143 2.3 Data collection

144 The data required by the SWAT model includes a digital elevation model (DEM), soil data, land
145 use, and hydrological and climate data (Table 1). The climate data were obtained from five weather
146 stations in the HID.

147 The water efficiency of the canal system in this model was obtained from local agricultural
148 administrations (AHID, 2015). To divide the sub-basins, we defined the drainage ditch as the stream
149 (AHID, 2015) and burn-in into the DEM, and the simulation results were verified by the discharge of
150 the drainage ditch.

151 The model generated 5 outlets and 73 sub-basins, and the measured data of the first outlet in the
152 study area was obtained. Therefore, this study chose the area controlled by this outlet as the study area.
153 The crops' yields (wheat, corn and sunflower) required for the calculation of the water footprint was
154 obtained from the Statistical Yearbook of the local agricultural administrations (AHID, 2015).

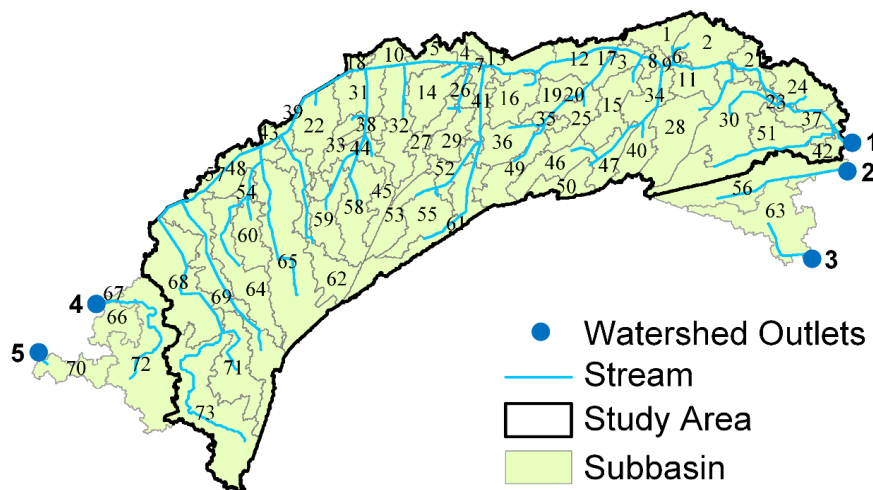
155 Table 1 Data used in the study and the resources.

Dataset	Data description	Resolution	Data sources
DEM	—	30×30 m	Geospatial Data Cloud (CAS, 2009a)
Soil	Soil type map, Soil physical and chemical properties	1:1000000	China Soil Scientific Database (CAS, 2009b)
Land use	—	1:100000 (2010)	Data Center for Resources and Environmental Sciences (CAS, 2010)



Weather	Precipitation, Wind speed,	Daily	China Meteorological Data Network
	Solar radiation,	(1980-2012)	(NMIC, 2015)
	Maximum temperature,		The Administration of Hetao Irrigation
	Minimum temperature,		District (AHID, 2015)
	Relative humidity		
Hydrologic	Stream map,	Monthly	The Administration of Hetao Irrigation
	Discharge	(2003-2012)	District (AHID, 2015)
Crop parameter data	Dates of plant and harvest,	—	The Administration of Hetao Irrigation
	Dates of irrigation,		District (AHID, 2015)
	Irrigation quota		

156



157

158

Fig. 2. Subbasins and study areas

159

2.4 Calibration and validation

160

The Sequential Uncertainty Fitting (SUFI-2) algorithm in SWAT-CUP was applied for calibration

161

and validation (Abbaspour et al., 2007; Abbaspour, 2012) by comparing the simulated stream discharge

162

from the model with the measured discharge data. The global sensitivity analysis integrated within

163

SUFI-2 was used to evaluate the hydrologic parameters for the discharge simulation and then the



164 optimal simulation is established by adjusting the sensitivity parameters and through multiple iterations.

165 The calibration period was from 2006-2009, and the validation period was from 2010-2012.

166 For calibration and validation analyses, the monthly measured discharges were compared with the
167 simulated discharge data and the model performance was evaluated using the coefficient of
168 determination (R^2), Nash efficiency coefficient (NSE) (Nash and Sutcliffe, 1970; Moriasi et al., 2007)
169 and percent deviation (PBIAS) (Gupta et al., 1999). The calculation formula is as follows:

$$170 \quad R^2 = \frac{\left[\sum_{i=1}^n (Q_m - \bar{Q}_m)(Q_s - \bar{Q}_s) \right]^2}{\sum_{i=1}^n (Q_m - \bar{Q}_m)^2 \sum_{i=1}^n (Q_s - \bar{Q}_s)^2} \quad (2)$$

$$171 \quad NSE = 1 - \frac{\sum_{i=1}^n (Q_m - Q_s)^2}{\sum_{i=1}^n (Q_m - \bar{Q}_m)^2} \quad (3)$$

$$172 \quad PBIAS = \frac{\sum_{i=1}^n (Q_m - Q_s)}{\sum_{i=1}^n Q_{m,i}} \times 100 \quad (4)$$

173 where Q_m is the measured data, \bar{Q}_m is the mean of the measured data, Q_s is the model
174 simulation data, and \bar{Q}_s is the mean of the model simulation data.

175 R^2 measures the simulated and measured values of goodness. The closer the value is to 1, the
176 higher the agreement is between the simulated and measured discharge. The NSE is widely applied in
177 hydrologic models that range from negative infinity to 1 with 1 being the ideal value. The PBIAS
178 assesses the average deviation of the simulated values from observed values with 0 as the ideal value,
179 and a positive (negative) PBIAS value shows an underestimation (overestimation) bias of the simulated
180 variable compared to the measured variable. The monthly model data simulation results can be
181 classified as satisfactory if $R^2 > 0.6$, $NSE > 0.5$ and $PBIAS < \pm 25$ and can then be used for further

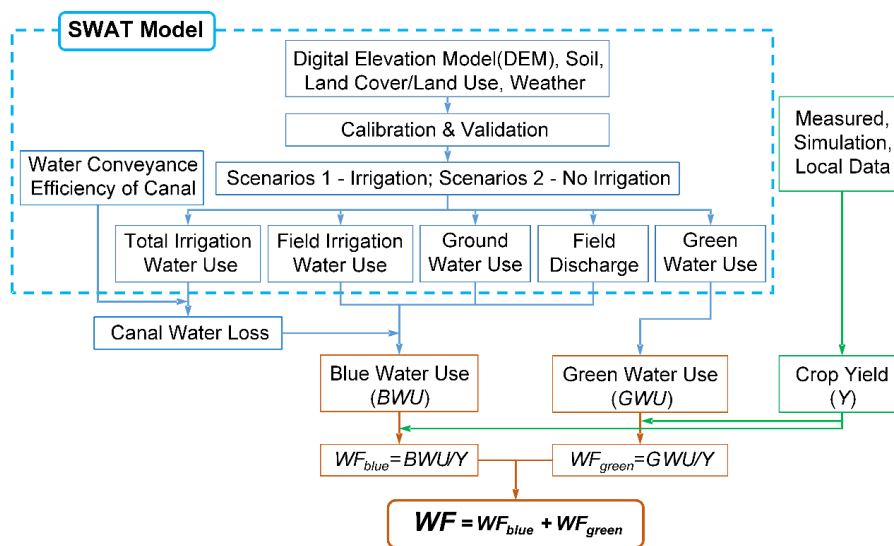


182 analysis (Moriassi et al., 2007).

183 The SWAT-CUP parameter sensitivity analysis procedure showed that the CN2, ESCO,
 184 GW_REVAP and ALPHA_BF parameters were more sensitive. In this study, the R2, NSE, and BIAS
 185 for the measured and calibration period were 0.77, 0.65 and 17, respectively; and the R2, NSE, and
 186 PBIAS for the validation period were 0.68, 0.61 and 21, respectively (Luan et al., 2018). The model
 187 simulation result can be classified as satisfactory (Moriassi et al., 2007). Therefore, the results
 188 demonstrated that the SWAT model was applicable in HID for future hydrologic process assessments.

189 2.5 The region-scale water footprint calculation method

190 Based on the water footprint theory framework provide by Hoekstra et al. (2011), this study
 191 suggests a new way of quantifying the region-scale water footprint of crop production (Fig. 3).



192

193 **Fig. 3.** The flowchart for calculating the region-scale water footprint

194 In this study, green water consumption is the ET produced by the consumption of precipitation
 195 during crop growth. Blue water consumption includes canal water loss during delivery, the ET
 196 produced by consumption of irrigation water and groundwater for crops growth, and the drainage in the



197 fields. To calculate the canal water loss, an extra model needs to be established according to the HID
198 situation, and the other can be simulated and obtained by the SWAT model.

199 **2.5.1 Calculation of water consumption factors in the fields**

200 Water consumption in the fields consists of 4 parts including the ET of precipitation, irrigation
201 water, groundwater utilized by crops, and field drainage. This study set up two scenarios and calculated
202 the above water consumption by changing the sources of water in the SWAT model. In scenario 1 (S1),
203 water consumption was derived from precipitation and irrigation water in the fields (irrigation systems
204 and irrigation quotas are based on local irrigation methods), i.e., the actual situation of crop water use.
205 In scenario 2 (S2), water consumption was only derived from precipitation without irrigation. In S1,
206 after calibration and validation of the model, and by modifying the crop water management data,
207 removing irrigation water, and simulating again, the results in S2 could be obtained. Then, the results
208 were calculated using two simulations, specifically, modifying the single variable to observe the
209 corresponding result. The calculation formula is as follows.

$$210 \quad WF = WF_g + WF_b = \frac{W_g}{Y} + \frac{W_b}{Y} \quad (5)$$

$$211 \quad W_g = ET_{s2} - Q_g \quad (6)$$

$$212 \quad W_b = Q_c + Q_f + Q_g + Q_d \quad (7)$$

$$213 \quad Q_c = I_i - I_f \quad (8)$$

$$214 \quad Q_f = ET_{s1} - W_g \quad (9)$$

215 where WF is the water footprint of crop production (m^3/t), WF_g is the green footprint (m^3/t), WF_b
216 is the blue water footprint (m^3/t), W_g is the green water consumption during the crop growth period
217 (m^3), W_b is the blue water consumption during the crop growth period (m^3), Y is the crop yield (t), ET_{s1}
218 is the crop actual ET during the crop growth period in Scenario 1 (m^3), ET_{s2} is the crop actual ET



219 during the crop growth period in Scenario 2 (m^3), Q_g is the amount of groundwater that rises to the soil
220 plow layer (m^3), Q_c is the amount of water loss in the canal system (m^3), Q_f is the ET of field irrigation
221 water (m^3), Q_d is the field discharge (m^3), I_t is the amount of total irrigation water diversion (m^3), and I_f
222 is the actual amount of water irrigated in the field (m^3).

223 **2.5.2 Calculation of water loss during delivery**

224 Water loss during transportation occurs in the canal and is an important part of blue water
225 consumption of the crops growth. Because of the complexity of the irrigation canal system and the lack
226 of hydrological data (lack of water conveyance efficiency of the branch canal and lower canal), we
227 generalized the irrigation area into a similar rectangle model (Fig. 4). Each rectangle is the area
228 controlled by each main canal, which is represented by the central line. The natural canal system is
229 divided into two parts when calculating the water loss of the canal system. Part A is the loss of the
230 general main canal and the main canals, and the part B is the loss of the rest of the canal system
231 including the branch canals, lateral canals, field canals, and sub-lateral canals.

232 The water loss in part A could be calculated as follows: divide the main canal by equidistance (10
233 km) and then calculate the water loss of each section, which was produced by local and downstream
234 water of which local water accounted for a small amount and the rest belonged to the downstream.
235 Therefore, the local accurate water loss should include this section and upstream sections. We assumed
236 local water loss to the midpoint of each canal. In ArcGIS, we used a Kriging interpolation to obtain the
237 water loss figure of part A.

238 Water loss in part B could be calculated as follows: the water loss of the other canals below the
239 main canal divided by the area controlled by each main canal and the water loss per unit area controlled
240 by the corresponding canal could be obtained. Then, the water loss per unit area controlled by each



241 main canal could be obtained. The data of parts A and B are calculated using the Space analysis tool in
242 ArcGIS 10.1 software to obtain the distribution map of the water loss in the drainage system.

243 The formulas are as follows:

$$244 \quad W_A = I_t \times (1 - k_g \times k_m) \quad (10)$$

$$245 \quad S_{ji} = \frac{S_j}{i} \quad (11)$$

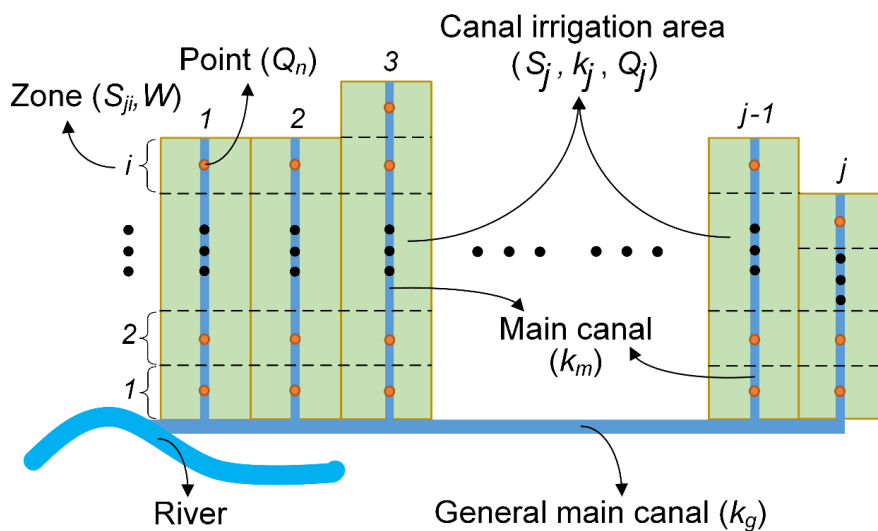
$$246 \quad W = \frac{W_A \times k_j}{i \times S_{ji}} \quad (12)$$

$$247 \quad Q_n = W \times \left(\frac{1}{i} + \frac{1}{i-1} + \frac{1}{i-2} + \dots + \frac{1}{i-(n-1)} \right) \quad n \in (1, 2, 3, \dots, i) \quad (13)$$

$$248 \quad W_B = Q_c - W_A \quad (14)$$

$$249 \quad Q_j = \frac{W_B \times k_j}{S_j} \quad (15)$$

250 where W_A is the amount of water loss in part A (m^3), I_t is the amount of total irrigation water diversion
251 (m^3), k_g is the water conveyance efficiency of the general main canal, k_m is the water conveyance
252 efficiency of the main canal, S_j is the area controlled by the j th main canal (ha), i is the number of the
253 equidistance section of the j th main canal, S_{ji} is the area per section controlled by the j th main canal
254 (ha), k_j is the ratio of the diversion volume of the j th main canal to the total diversion, W is the water
255 loss per unit area of the section of the j th main canal in part A (m^3/ha), Q_n is actual the amount of water
256 loss per unit area of the section of the j th main canal (m^3/ha), W_B is the amount of water loss in part B
257 (m^3), and Q_j is the water loss per unit area of the j th main canal (m^3/ha).



258

259

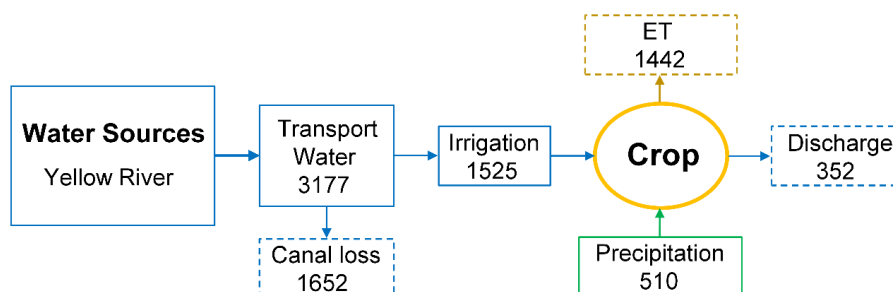
Fig. 4. Generalized model of the irrigation area

260 **3 Results**

261 **3.1 Analysis of the process of crop production and the quantification of hydrological**

262 **elements in each link**

263 Fig. 5 shows the average water input and consumption of the study area in the process of water
 264 diversion, transportation, irrigation and drainage from 2006 to 2012. In HID, the water input for
 265 irrigation for the three crops in the study area was 3177 Mm³, water loss during transportation in the
 266 canals was 1652 Mm³, the actual field irrigation water was 1525 Mm³, precipitation in the farmland
 267 was 510 Mm³, the actual ET of the farmland was 1442 Mm³, the discharge was 352 Mm³, and the
 268 groundwater was not considered because the consumption was less than 5%. When inputting water into
 269 the farmland, irrigation and precipitation accounted for 74.9% and 25.1%, respectively; however, when
 270 consuming water, the discharge took up 47.9%, 41.8% and 10.3%, respectively. Irrigation was the main
 271 water source in the irrigated district, and the water loss in the canals and actual ET were the main water
 272 output in the irrigated district.



273

274

Fig. 5. The amount of water during crop growth (Mm³)

275

276

277

278

279

280

281

282

283

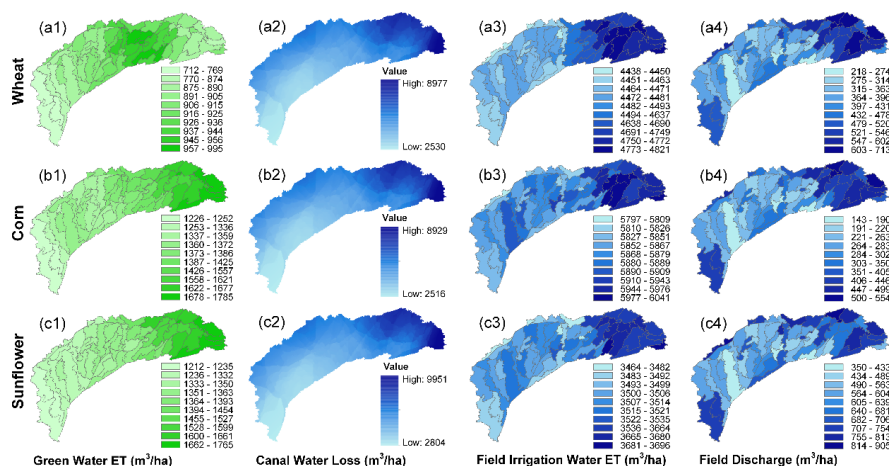
284

285

286

287

Green water is the precipitation used for crop growth; therefore, the green water footprint is highly correlated with precipitation in its growth period. Wheat's growth period is from April to July, whereas that of corn and sunflower is from May to September. During the growth period of wheat, the mean precipitation from 2006 to 2012 was 108.9 mm, and for corn and sunflower, the corresponding mean precipitation was 176.1 mm. The green footprint of wheat during the growth period was lower than that of corn and sunflower because of the lower mean precipitation in the wheat growth period. The green water consumption of corn was close to the value of sunflower. The green water consumption of wheat, corn and sunflower were 895 m³ ha⁻¹, 1441 m³ ha⁻¹ and 1419 m³ ha⁻¹ (Fig. 6 a1, b1, c1), respectively. Meanwhile, green water consumption in the high precipitation area was larger, for instance, the precipitation during the wheat growth period in Wuyuan reached 116.3 mm, and the green water consumption in this region was the largest (up to 995 m³ ha⁻¹). In the growth period of corn and sunflower, the precipitation in Wulateqianqi reached 199.4 mm, and the green water consumption in this area was again the largest, reaching 1785 m³ ha⁻¹ and 1765 m³ ha⁻¹, respectively.



288

289

Fig. 6. Spatial distribution of the different water consumption of three crops ($\text{m}^3 \text{ha}^{-1}$)

290

291

292

293

294

295

296

297

298

299

300

301

302

303

Blue water is surface water and groundwater used for crop growth. In blue water consumption, the farther away from the watershed inlets the longer the canal was and the larger the water loss of the three crops. Northeast of the irrigation area (parts of Wuyuan and Wulateqianqi) and due to the far distance from watershed inlets, canal water loss in these places was much higher than that in other areas, and the maximum canal water loss of wheat, corn and sunflower reached $8977 \text{ m}^3 \text{ha}^{-1}$, $8929 \text{ m}^3 \text{ha}^{-1}$ and $9951 \text{ m}^3 \text{ha}^{-1}$, respectively. The different amount of canal water loss was caused by the difference of water loss in the unit area, at $4778 \text{ m}^3 \text{ha}^{-1}$, $4753 \text{ m}^3 \text{ha}^{-1}$ and $5297 \text{ m}^3 \text{ha}^{-1}$, respectively.

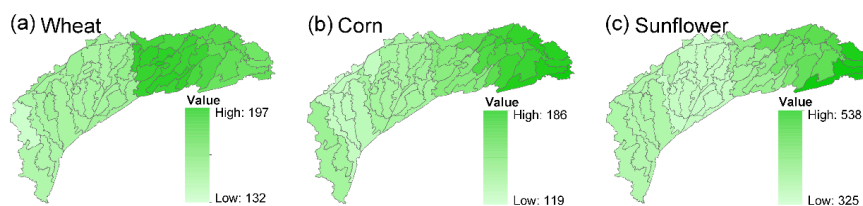
The actual ET and the discharge of the three crops was higher in the east than in the west, which was due to the higher evaporation in the east than in the west. Meanwhile, Fig. 6 shows that the actual ET in the field was complementary with discharge. The higher the actual ET, the smaller the discharge and vice versa.

3.2 The regional green water footprint of crop production

The green water footprint of the crops is produced by precipitation during crop growth. The spatial difference of the green water footprints of wheat, corn and sunflower in HID was obvious (Fig. 7). It



304 can be seen from the figure that the overall distribution of the green water footprint of the three crops
305 was higher in the east than it was in the west. However, the distribution of green water footprints was
306 somewhat different for each crop. Wheat had the largest green water footprint in Wuyuan ($197 \text{ m}^3 \text{ t}^{-1}$)
307 and the lowest in Dengkou ($132 \text{ m}^3 \text{ t}^{-1}$). Corn had the largest green water footprint in Wulateqianqi (186
308 $\text{m}^3 \text{ t}^{-1}$) and the lowest in Hangjinhouqi ($119 \text{ m}^3 \text{ t}^{-1}$), but in Dengkou, it was approximate to that in Linhe,
309 ranging from 133 to $139 \text{ m}^3/\text{t}$. Sunflower had the largest green water footprint in Wulateqianqi (538 m^3
310 t^{-1}) and the lowest in Linhe ($325 \text{ m}^3 \text{ t}^{-1}$). The green water footprint of crop production also varied across
311 crops. The largest average green water footprint in HID was sunflower, followed by wheat and corn.



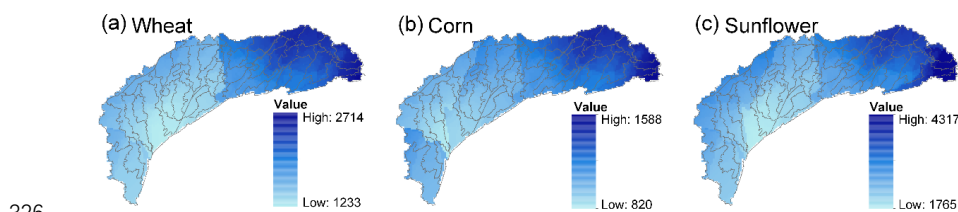
313 **Fig. 7.** The spatial distribution of the green water footprint of crop production in the HID ($\text{m}^3 \text{ t}^{-1}$)

314 **3.3 The regional blue water footprint of crop production**

315 The blue water footprint of the crops is produced by blue water that is consumed during crop
316 growth. The blue water consumption during crop growth mainly includes the loss during transportation,
317 ET and field drainage. Fig. 8 shows the spatial variability of wheat, corn, and sunflower in HID. The
318 overall distribution of the total water footprint of the three crops was higher in the east than in the west
319 and higher in the north than in the south. However, the specific distribution was somewhat different for
320 each crop. Wheat had the largest blue water footprint in Wulateqianqi ($2714 \text{ m}^3 \text{ t}^{-1}$) and the lowest in
321 southern Linhe ($1233 \text{ m}^3 \text{ t}^{-1}$). Corn had the largest blue water footprint in northern Wulateqianqi (1588
322 $\text{m}^3 \text{ t}^{-1}$) and the lowest in southern Hangjinhouqi ($820 \text{ m}^3 \text{ t}^{-1}$). Sunflower had the largest blue water
323 footprint in northern Wulateqianqi ($4317 \text{ m}^3 \text{ t}^{-1}$) and the lowest in southern Linhe ($4317 \text{ m}^3 \text{ t}^{-1}$). The



324 blue water footprint of crop production also varied across crops. The largest of the average blue water
325 footprint in the HID was sunflower, followed by wheat and corn.

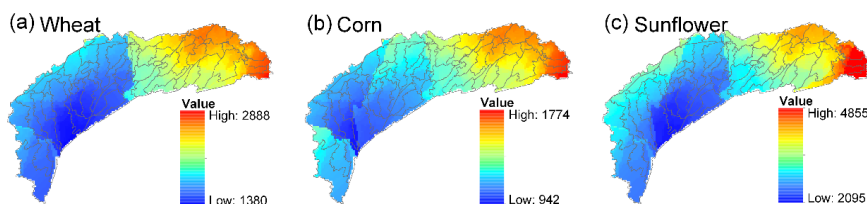


326

327 **Fig. 8.** The spatial distribution of the blue water footprint of crop production in the HID ($\text{m}^3 \text{t}^{-1}$)

328 **3.4 The regional total water footprint of crop production**

329 The total water footprint of crop production consists of both blue and green water footprints
330 during the crop growth period. Fig. 8 shows the total water footprint of crop production and spatial
331 variability of wheat, corn, and sunflower in HID. The overall distribution of the total water footprint of
332 the three crops was higher in the east (Wulateqianqi and Wuyuan) than it was in the west (Dengkou),
333 followed by the central region (Hangjinhouqi and Linhe) and was higher in the north than in the south.
334 However, the specific distribution was somewhat different for each crop. Wheat had the largest total
335 water footprint in the east (Wulateqianqi, $2888 \text{ m}^3 \text{ t}^{-1}$) and the lowest in southern Linhe ($1380 \text{ m}^3 \text{ t}^{-1}$).
336 Corn had the largest total water footprint in the east (Wulateqianqi, $1774 \text{ m}^3 \text{ t}^{-1}$) and the lowest in
337 southern Hangjinhouqi ($942 \text{ m}^3 \text{ t}^{-1}$). Sunflower had the largest total water footprint in the east
338 (Wulateqianqi, $4885 \text{ m}^3 \text{ t}^{-1}$) and the lowest value was in southern Linhe ($2095 \text{ m}^3 \text{ t}^{-1}$). The total water
339 footprint of crop production also varied across crops. The largest of the average total water footprint in
340 the HID was sunflower, followed by wheat and corn. The blue water footprint of wheat, corn and
341 sunflower accounted for 89%, 87% and 86% of the total water footprint, respectively.



342

343 **Fig. 9.** The spatial distribution of the total water footprint of crop production in the HID (m³/t)

344 **4 Discussion**

345 **4.1 Methods of calculating crop production water footprints——region scale and field scale**

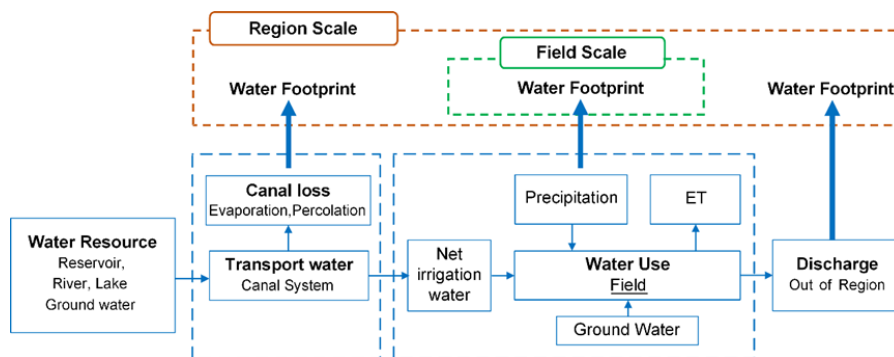
346 In this paper, the calculation method of calculating crop production water footprints is divided into
347 the field and region scales, according to the calculation boundary of water consumption in crop growth.

348 The field-scale water footprint is composed of the transpiration of crops and the evaporation of
349 soil, and the water loss during transportation is not included. Current studies had different geographical
350 scales, such as a global scale (Mekonnen and Hoekstra, 2011), a national scale, such as Europe
351 (Vanham and Bidoglio, 2013) and China (Zhao, 2009), and a regional scale, such as Beijing (Sun,
352 2013a), Cremona province (Bocchiola, 2015) and Hetao (Luan et al., 2018); however, they all
353 calculated the crop production water footprint of the field scale. These studies were based on empirical
354 formulas, which could be divided into two methods. The first method is the irrigation schedule method,
355 such as CROPWAT (Mekonnen and Hoekstra, 2011), CropSyst (Bocchiola et al., 2013), the EPIC
356 model (Williams et al., 1989; Shi et al., 2017), the GEPIC model (Liu et al., 2007), and the
357 AQUACROP model (Chukalla, 2015; Zhuo 2016). The other method is the crop water requirement
358 method (Cao et al., 2014; Sun et al., 2013c). The calculation of crop ET in these methods was based on
359 the full satisfaction of the crop water requirement, there is no water deficit, and the actual soil water
360 content was not taken into consideration. Therefore, the results did not reflect the actual water
361 consumption of the crops, and the water footprint of the crop production in the field scale cannot



362 distinguish the source of blue water consumption from the surface water or groundwater.

363 The region-scale water footprint calculation method considered all of the water consumption
364 related to crop growth from the water source to the field. It not only included the ET from the field but
365 also the water loss during transportation in the canal system and the water loss discharged out of the
366 region. The blue water was consumed for crop growth and thus had to be included in the calculation of
367 the water footprint. This was also the definition of crop water consumption in the crop production
368 water footprint concept, which included all of the processes related to crop production, such as storage
369 and transportation (the water that ran to other basins or seas such as the discharge out of the region
370 instead of running back to the former basin) (Hoekstra, et al., 2011). The water footprints of the whole
371 area irrigated by the canal system could be calculated by the region-scale method. To date, few studies
372 have examined a region-scale water footprint. Sun et al. (2013b) calculated the regional water footprint
373 in HID; however, the calculation was merely based on the principle of water balance and calculated the
374 blue water consumption of the whole region based on the difference of water diversion and discharge in
375 the region without distinguishing the specific parts of blue water loss.



376

377

Fig. 10. The different scales of calculating water footprints

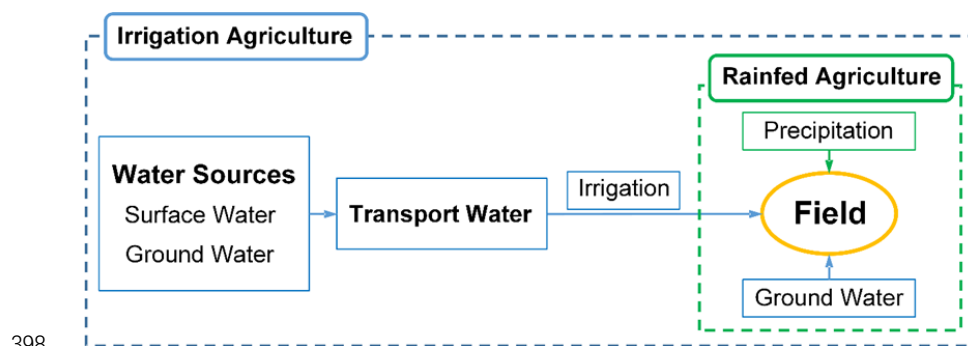
378

4.2 Comparison of the applicability of two methods



379 The applicable conditions of the two methods of calculating water footprints are different. In
380 terms of the calculation boundary, the calculation of the green water footprint is the same, whereas the
381 calculations of the blue water footprint are different. Fig. 11 illustrates the water sources and use
382 conditions of two types of agriculture. The rainfed agriculture depends on precipitation (green water)
383 and groundwater (blue water), and the water consumption mainly includes ET. While irrigation
384 agriculture relies on surface water, groundwater and precipitation, water consumption includes ET,
385 transport loss and discharge. Therefore, the field-scale method is suitable for calculating the water
386 footprint of rainfed agriculture, whereas the region-scale method applies to the calculation of the
387 irrigation agriculture water footprint.

388 Currently, irrigated farmland occupies 39.6% of the total arable land in China (NBSC, 2016).
389 Globally, irrigated area accounts for 20.6% of all arable land (FAO, 2016). Overall, the yields of
390 irrigation agriculture are much higher than that of rainfed agriculture. If the water footprints of
391 irrigation agriculture are calculated by the field-scale method without considering water loss during
392 transportation or discharge, the calculated values are smaller than the actual values, and the actual
393 water footprints of irrigation agriculture cannot be precisely assessed. This is also the deficiency of the
394 current crop production water footprint studies because most studies have adopted the field-scale
395 method. Therefore, using the region-scale method to calculate the crop water footprint, especially in
396 irrigation agriculture, is the basis for a comprehensive and accurate evaluation of a crop production
397 water footprint in China and other regions or countries.



398

399

Fig. 11. Irrigation agriculture and rainfed agriculture

400 4.3 The methods of calculating region-scale crop production water footprints

401 In this study, we proposed an improved calculation method of the region-scale crop production
402 water footprint. The method based on the hydrological model (SWAT model), which used the irrigation
403 canal water use coefficient, calculated all of the water consumption in the process of crop growth by
404 area (Hetao irrigation area) such as green water consumption, blue water in conveying process
405 consumption, and irrigation and drainage in the field. The SWAT model could be used to simulate the
406 regional hydrologic cycle and its simulation results could calculate the water use process during the
407 crop growth period such as irrigation, precipitation, groundwater, ET and drainage. Then, combined
408 with the water conveyance efficiency of the canal, the water canal loss during transportation could be
409 calculated. In addition, this method could calculate the use of groundwater during the crop growth
410 period, and therefore, blue water could be divided into surface water and groundwater for an additional
411 accurate analysis of water sources for crop growth. To date, many scholars have conducted a few
412 corresponding studies (Mekonnen and Hoekstra, 2010). Therefore, this method can calculate water use
413 during the crop growth period and then more precisely calculate the blue, green and total crop water
414 footprints.

415 In HID, the canal water loss accounted for 47.9% of all water consumption, which is one of the



416 main water consumption components during the crop growth period. Therefore, it is necessary to
417 calculate the crop water footprints in irrigated areas using the regional scale. The water footprints of
418 three crops (wheat, corn and sunflower) in HID and calculated by this method are 1380-2888 m³ t⁻¹,
419 942-1774 m³ t⁻¹, and 2095-4855 m³ t⁻¹, respectively. These values are higher than the results calculated
420 by the field-scale method. Cao et al. (2014) calculated the mean crop water footprints of China
421 irrigation agriculture from 1998 to 2010 in which the mean total water footprint of many crops in the
422 Inner Mongolia autonomous region (including HID) was 1556 m³ t⁻¹. Sun et al. (2013b) used the
423 region-scale method and the water balance principle to calculate the average water footprint of HID
424 and it was 3.91 m³ kg⁻¹ in which blue water accounted for 90.9% and green water accounted for 9.1%.
425 This result was the average water footprint of many crops, and the value was approximate to our results
426 for the blue water of wheat, corn and sunflower and accounted for 89%, 87% and 86%, respectively.
427 However, Sun et al. (2013b) could not distinguish each crop or illustrate the difference of spatial
428 distribution.

429 The region-scale method proposed in this paper not only applies to water footprints of irrigation
430 agriculture but also applies to the calculation of rainfed agriculture. If there is only natural precipitation
431 without irrigation in the study area, irrigation can be excluded in the SWAT model to simulate the water
432 circle in the field with rainfed conditions to calculate the field-scale water footprints of crop production.
433 Therefore, this study method is suitable for two scales.

434 There are limitations to this approach. The method needs more data types (for instance, DEM,
435 land use, soil and climate data, hydrological data, and crop management), and high-precision data is
436 required, which are difficult to obtain. This method does not apply to areas without the above data.

437 **5 Conclusions**



438 In this study, we proposed an improved region-scale method for calculating crop water footprints.
439 This method is based on the hydrological model (SWAT model), combined the irrigation parameters of
440 the irrigation area (water conveyance efficiency of canal), and calculated the crop production water
441 footprints.

442 The method can analyze the process of water use during the crop growth period, including
443 irrigation precipitation, groundwater, ET and drainage, for a more comprehensive calculation of water
444 consumption during the crop growth period and more precisely quantify crop production water
445 footprints. The method can be applied to calculate the crop production water footprint at both the field
446 and region scale. In HID, the main water consumption occurs during the crop growth period; the canal
447 water loss was 1652 Mm³ and ET in the field was 1442 Mm³, which accounted for 47.9% and 41.8% of
448 the total consumption, respectively.

449 Based on this method, the total water footprints of three crops (wheat, corn and sunflower) in HID
450 were 1380-2888 m³ t⁻¹, 942-1774 m³ t⁻¹, and 2095-4855 m³ t⁻¹. In terms of spatial distribution, the
451 values were higher in the east than they were in the west. The spatial distributions of blue and green
452 water footprints were similar, and the blue water footprint accounted for more than 86% of the total
453 water footprint.

454 Green water consumption was directly related to precipitation in the crop growth period. Less
455 precipitation in the growth period of wheat led to less green water consumption and blue water
456 consumption accounted for 93.1%. For corn and sunflower, blue water consumption accounted for 89.7%
457 and 90.1%, respectively. For blue water consumption, water loss during transportation increased with
458 the increasing distance of the canals, and the farther away from the watershed inlets they were, the
459 more water was lost.



460 **Acknowledgements:**

461 This work is jointly supported by the National Natural Science Foundation of China (51409218;
462 51609063), the National Key Research and Development Program of China (2016YFC0400201), and
463 Science and Technology Integrated Innovation Project, Shaanxi Province of China
464 (2016KTZDNY-01-01), the Open Research Fund of the State Key Laboratory of Simulation and
465 Regulation of Water Cycle in River Basin at the China Institute of Water Resources and Hydropower
466 Research (IWHR-SKL-201601) and Young Scholar Project of Cyrus Tang Foundation.

467 **Author Contributions:** Pute Wu, Shikun Sun and Yubao Wang designed the study. Xiaobo Luan, Yali
468 Yin and Jing Liu did the literature search and data collection. Shikun Sun, Xiaobo Luan and Xuerui
469 Gao managed and analyzed the data. Suikun Sun and Xiaobo Luan drew the figures and wrote the
470 paper. All authors discussed and commented on the manuscript.



471 **References:**

- 472 Abbaspour, K. C. (2012). SWAT-CUP 2012: SWAT Calibration and Uncertainty Programs - A User
473 Manual. Eawag: Swiss Federal Institute Science and Technology.
- 474 Abbaspour, K. C., Vejdani M., & Haghighat S. (2007). SWAT-CUP calibration and uncertainty
475 programs for SWAT. Modsim 2007: International Congress on Modelling and Simulation: Land,
476 Water and Environmental Management: Integrated Systems for Sustainability. Christchurch, New
477 Zealand.
- 478 AHID, (2015). The Administration of Hetao Irrigation District (AHID), Bayannaoer Department of
479 Water, Inner Mongolia Autonomous Region, China (<http://www.htgq.gov.cn/>).
- 480 Allen, R. G., Pereira, L. S., Raes, D., & Smith, M. (1998). Crop evapotranspiration: Guidelines for
481 computing crop water requirements. FAO Irrigation and Drainage Paper 56, Rome.
- 482 Arnold, J. G., Srinivasan, R., Muttiah, R. S., & Williams, J. R. (1998). Large area hydrologic modeling
483 and assessment part I: model development. Journal of the American Water Resources Association,
484 34(1), 91-101.
- 485 Bao, C., Fang, C. (2012). Water Resources Flows Related to Urbanization in China: Challenges and
486 Perspectives for Water Management and Urban Development. Water Resources Management,
487 26(2), 531-552.
- 488 Bocchiola, D. (2015). Impact of potential climate change on crop yield and water footprint of rice in
489 the Po valley of Italy. Agricultural Systems, 139, 223-237.
- 490 Bocchiola, D., Nana, E., & Soncini, A. (2013). Impact of climate change scenarios on crop yield and
491 water footprint of maize in the Po valley of Italy. Agricultural Water Management, 116(2), 50-61.
- 492 Cao, X., Wu, P., Wang, Y., & Zhao, X. (2014). Water Footprint of Grain Product in Irrigated Farmland



- 493 of China. *Water Resources Management*, 28(8), 2213-2227.
- 494 CAS, (2009a). Geospatial Data Cloud site (GSCloud), Computer Network Information Center, Chinese
495 Academy of Sciences (<http://www.gscloud.cn>).
- 496 CAS, (2009b). China Soil Scientific Database (CSDB), Soil Research Center, Institute of Soil Science,
497 Chinese Academy of Sciences (<http://www.soil.csdb.cn/>).
- 498 CAS, (2010). Data Center for Resources and Environmental Sciences (RESDC), Chinese Academy of
499 Sciences (<http://www.resdc.cn>).
- 500 Chen, J. (2007). Rapid urbanization in China: a real challenge to soil protection and food security.
501 *Catena*, 69(1), 1-15.
- 502 Chukalla, A. D., Krol, M. S., & Hoekstra, A. Y. (2015). Green and blue water footprint reduction in
503 irrigated agriculture: effect of irrigation techniques, irrigation strategies and mulching. *Hydrology
& Earth System Sciences*, 12(7), 6945-6979.
- 505 Deng, X. P., Shan, L., Zhang, H., & Turner, N. C. (2006). Improving agricultural water use efficiency
506 in arid and semiarid areas of China. *Agricultural Water Management*, 80(1), 23-40.
- 507 Du, T., Kang, S., Zhang, X., & Zhang, J. (2014). China's food security is threatened by the
508 unsustainable use of water resources in North and Northwest China. *Food and Energy Security*,
509 3(1), 7-18.
- 510 Duh, J., Shandas, V., Chang, H., & George, L. A. (2008). Rates of urbanisation and the resiliency of air
511 and water quality. *Science of The Total Environment*, 400(1-3), 238-256.
- 512 Elliott, J., Deryng, D., Muller, C., Frieler, K., Konzmann, M., Gerten, D., et al. (2014). Constraints and
513 potentials of future irrigation water availability on agricultural production under climate change.
514 *Proceedings of the National Academy of Sciences of the United States of America*, 111(9),



- 515 3239-3244.
- 516 FAO. 2016. AQUASTAT website. Food and Agriculture Organization of the United Nations (FAO).
517 Website accessed on [2017/9/20].
- 518 FAO. 2010. Food and Agriculture Organization of the United Nations, Land and Water Development
519 Division. CROPWAT model. Rome, Italy: Food and Agriculture Organization;
520 (<http://www.fao.org/land-water/databases-and-software/cropwat/en/>).
- 521 Fu, G., Chen, S., Liu, C., & Shepard, D. (2004). Hydro-climatic trends of the Yellow River basin for
522 the last 50 years. *Climatic Change*, 65, 149-178.
- 523 Gupta, H. V., Sorooshian, S., Yapo, P. O., Gupta, H. V., & Yapo, P. O. (1999). Status of automatic
524 calibration for hydrologic models: comparison with multilevel expert calibration. *Journal of*
525 *Hydrologic Engineering*, 4(2), 135-143.
- 526 Haddeland, I., Heinke, J., Biemans, H., Eisner, S., Flörke, M., Hanasaki, N., et al. (2014). Global water
527 resources affected by human interventions and climate change. *PNAS*, 111(9), 3251-3256.
- 528 Haverkamp, S., Srinivasan, R., Frede, H. G., & Santhi, C. (2002). Subwatershed spatial analysis tool:
529 discretization of a distributed hydrologic model by statistical criteria. *Journal of the American*
530 *Water Resources Association*, 38, 1723-1733.
- 531 Hoekstra, A. Y. (ed) (2003) 'Virtual water trade: Proceedings of the International Expert Meeting on
532 Virtual Water Trade', 12-13 December 2002, Value of Water Research Report Series No 12,
533 UNESCO-IHE, Delft, Netherlands, <http://waterfootprint.org/media/downloads/Report12.pdf>
- 534 Hoekstra, A. Y., Chapagain, A. K., Aldaya M. M., & Mekonnen M. M. (2011). The water footprint
535 assessment manual-setting the global standard. London • Washington: Enschede.
- 536 Jiang, Y. (2009). China's water scarcity. *Journal of Environmental Management*, 90(11), 3185-3196.



- 537 Khan, S., Hanjra, M. A., & Mu, J. X. (2009). Water management and crop production for food security
538 in China: a review. *Agricultural Water Management*, 96(3), 349-360.
- 539 Liu J, Williams J. R, Zehnder A. J. B, & Yang H. (2007). GEPIC-modelling wheat yield and crop water
540 productivity with high resolution on a global scale. *Agricultural Systems*, 94(2):478-493.
- 541 Liu, J., Yang, H., & Savenije, H. H. (2008). China's move to higher-meat diet hits water security.
542 *Nature*, 454(7203), 555-561.
- 543 Luan X. B., Wu P. T., Sun S. K., Wang Y. B., Gao X. R. (2018). Quantitative study of the crop
544 production water footprint using the SWAT model. *Ecological Indicators*.89: 1-10.
- 545 Mekonnen, M. M., Hoekstra, A. Y., & Becht, R. (2012). Mitigating the Water Footprint of Export Cut
546 Flowers from the Lake Naivasha Basin, Kenya. *Water Resources Management*, 26(13),
547 3725-3742.
- 548 Mekonnen, M.M., & Hoekstra, A. Y. (2011). The green, blue and grey water footprint of crops and
549 derived crop products. *Hydrology & Earth System Sciences*, 15(5), 1577-1600.
- 550 Moriasi, D. N., Arnold, J. G., Liew, M. W. V., Bingner, R. L., Harmel, R. D., & Veith, T. L. (2007).
551 Model evaluation guidelines for systematic quantification of accuracy in watershed simulations.
552 *Transactions of the ASABE*, 50(3), 885-900.
- 553 Nash J. E., & Sutcliffe J. V. (1970). River flow forecasting through conceptual models Part I: A
554 discussion of principles. *Journal of Hydrology*, 10, 282-290.
- 555 NBSC. (2016). *China Statistical Yearbook 2016*. China Statistics Press, Beijing.
- 556 Neitsch, S. L., Arnold, J. G., Kiniry, J. R., & Williams, J. R., (2011). *Soil and Water Assessment Tool:*
557 *Theoretical Documentation, Version 2009*. Texas Water Resources Institute.
- 558 Nijssen, B., Odonnell, G. M., Hamlet, A. F., & Lettenmaier, D. P. (2001). Hydrologic Sensitivity of



- 559 Global Rivers to Climate Change. *Climatic Change*, 50, 143-175.
- 560 NMIC, (2015). China meteorological data network (CMA), National Meteorological Information
561 Center, China (<http://data.cma.cn/>).
- 562 Pasquale, S., Theodoresc, H., Dirk, R., & Elias, F. (2009). Aquacrop--the fao crop model to simulate
563 yield response to water: I. concepts and underlying principles. *Agronomy Journal*, 101(3),
564 448-459.
- 565 Piao, S., Ciais, P., Huang, Y., Shen, Z., Peng, S., Li, J., et al. (2010). The impacts of climate change on
566 water resources and agriculture in China. *Nature*, 467(7311), 43-51.
- 567 Schwarzenbach, R. P., Egli, T., Hofstetter, T. B., Von Gunten, U., & Wehrli, B. (2010). Global Water
568 Pollution and Human Health. *Annual Review of Environment and Resources*, 35(1), 109-136.
- 569 Shi, R., Ukaew, S., Archer, D. W., Lee, J. H., Pearlson, M. N., Lewis, K. C., et al. (2017). Life cycle
570 water footprint analysis for rapeseed derived jet fuel in North Dakota. *ACS Sustainable Chemistry
571 & Engineering*, 5(5), 3845-3854.
- 572 Shiklomanov I. A. (2000). Appraisal and assessment of world water resources. *Water International*,
573 25(1), 11-32.
- 574 Sun S. K., Wu P. T., Wang Y. B., & Zhao X. N. (2013c). The virtual water content of major grain crops
575 and virtual water flows between regions in China. *Journal of the Science of Food & Agriculture*,
576 93(6), 1427-37.
- 577 Sun S. K., Wu P.T., Wang Y. B., & Zhao X. N. (2013a). Temporal variability of water footprint for
578 maize production: the case of Beijing from 1978 to 2008. *Water Resources Management*, 27(7),
579 2447-2463.
- 580 Sun S. K., Wu P.T., Wang Y. B., Zhao X. N., Liu J., & Zhang X. (2013b). The impacts of inter-annual



- 581 climate variability and agricultural inputs on water footprint of crop production in an irrigation
582 district of China. *Science of the Total Environment*, 444(2), 498-507.
- 583 USDA (United States Department of Agriculture) (1994) 'The major world crop areas and climatic
584 profiles', *Agricultural Handbook No 664*, World Agricultural Outlook Board, USDA,
585 www.usda.gov/oce/weather/pubs/Other/MWCACP/MajorWorldCropAreas.pdf.
- 586 Vanham, D., & Bidoglio, G. (2013). A review on the indicator water footprint for the EU28. *Ecological
587 Indicators*, 26(3), 61-75.
- 588 Vörösmarty, C. J., McIntyre, P. B., Gessner, M. O., Dudgeon, D., Prusevich, A., Green, P., et al. (2010).
589 Global threats to human water security and river biodiversity. *Nature*, 467(7315), 555-561.
- 590 Wang, Y. B., Wu, P.T., Zhao, X. N., & Engel, B. A. (2014). Virtual water flows of grain within China
591 and its impact on water resource and grain security in 2010. *Ecological Engineering*, 69(69),
592 255-264.
- 593 Williams J. R., Jones C. A., Kiniry J. R., & Spanel D. A. (1989). The EPIC crop growth-model.
594 *Transactions of the ASABE*, 32(2), 497-511.
- 595 Zhao, X., Chen, B., & Yang, Z. F. (2009). National water footprint in an input-output framework - a
596 case study of China 2002. *Ecological Modelling*, 220(2), 245-253.
- 597 Zhuo, L., Mekonnen, M. M., & Hoekstra, A. Y. (2016). Benchmark levels for the consumptive water
598 footprint of crop production for different environmental conditions: a case study for winter wheat
599 in China. *Hydrology & Earth System Sciences Discussions*, 20(11), 4547-4559.